European Conference on Computational Fluid Dynamics
ECCOMAS CFD 2006
P. Wesseling, E. Oñate and J. Périaux (Eds)

REAL-TIME REDUCED BASIS TECHNIQUES FOR NAVIER-STOKES EQUATIONS: OPTIMIZATION OF PARAMETRIZED BYPASS CONFIGURATIONS

Gianluigi Rozza[*,1]

[*] MIT - Massachusetts Institute of Technology, Department of Mechanical Engineering
Room 3-264, 77 Massachusetts Avenue, MA-02139 Cambridge (USA)
e-mail: rozza@mit.edu
http://iacs.epfl.ch/∼rozza/

Key words: Design of improved biomechanical devices, parametrized PDEs, Navier-Stokes equations, reduced basis methods, bypass optimization, haemodynamics.

Abstract. *The reduced basis method on parametrized domains is applied to approximate blood flow through an arterial bypass. The aim is to provide (a) a sensitivity analysis for relevant geometrical quantities of interest in bypass configurations and (b) rapid and reliable prediction of integral functional outputs (such as fluid mechanics indexes). The goal of this investigation is (i) to achieve design indications for arterial surgery in the perspective of future development for prosthetic bypasses, (ii) to develop numerical methods for optimization and design in biomechanics, and (iii) to provide an input-output relationship led by models with lower complexity and computational costs than the complete solution of fluid dynamics equations by a classical finite element method.*

1 INTRODUCTION

When a coronary artery is affected by a stenosis, the heart muscle cannot be properly oxygenated through blood. Aorto-coronaric anastomosis restores the oxygen amount through a bypass surgery downstream an occlusion (see Figs. 1 and 2). At present, different kind and shape of aorto-coronaric bypasses are available and, consequently, different surgery procedures can be devised to set up a bypass. Numerical simulation of physiological flows allows better understanding of phenomena involved in coronary diseases (see [1]) and a potential reduction of surgical and post-surgical failures. It may also suggest new means in bypass surgical procedures as well as with less invasive methods to devise improved bypass configuration ([2], [3], [4]). Efficient schemes for reduced-basis techniques

[1]PhD ECCOMAS Award 2005. This work has been carried out in collaboration with Prof. A. Quarteroni of EPFL and Politecnico di Milano and Prof. A. Patera of MIT as a part of the research done for my PhD thesis. European Union Research Training Network "Haemodel" (HPRN-CT-2002-00270) and Swiss National Science Foundation (PBEL 2-111646) are kindly acknowledged.

[5] applied to parametrized partial differential equations (P^2DEs) have been developed to provide useful and real time indications (outputs) in a repetitive design environment as optimization requires and a sensitivity analysis on important geometrical quantities such as bypass diameter t, arterial diameter D, stenosis length S, graft angle θ, bypass bridge height H, shown in Fig.(1). In Fig. (2) we show an example of numerical simulation (velocity) of blood flow inside a bypass configuration. See [6] for a more general framework.

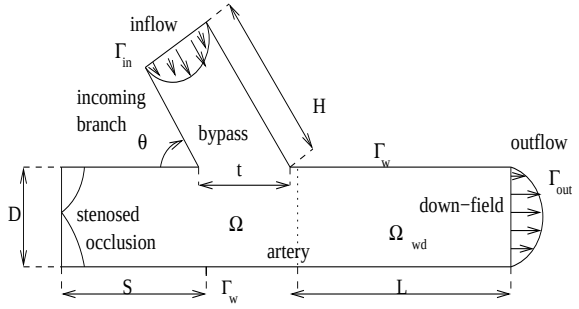

Figure 1: Bypass geometrical configuration, parametrized by H, L, S, t, D, θ.

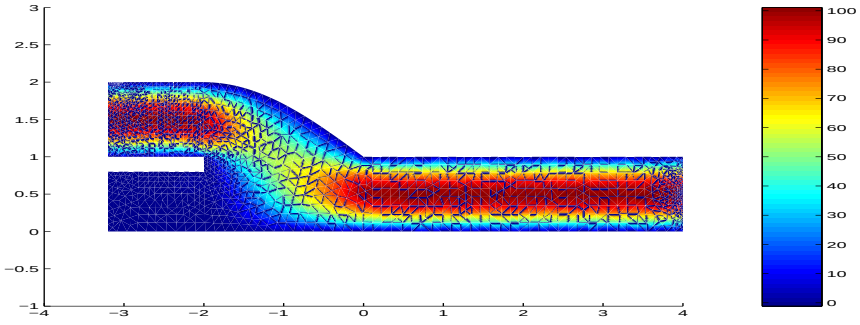

Figure 2: Idealized 2-D bypass configuration: iso-velocity $[ms^{-1} \cdot 10^{-2}]$.

1.1 Reduced basis methods for pre-process and real time optimization

Especially in the field of optimization and design, where the evaluation of many different possible configurations is required – corresponding to different choices of the design parameters – even for modest-complexity problems, the computational cost is unacceptably high. To more efficiently utilize the existing computational resources, reliable methods that reduce the complexity of the problem while at the same time preserve all relevant information, are becoming very important.
Central to every design, optimization, or control problem is the evaluation of an "input-output" relationship. The set of input parameters μ, which we will collectively denote as

"inputs," identify a particular configuration of the system or of one of its components. These inputs may represent design or decision variables, such as geometry or physical properties – for example, control variables in optimization studies. The output parameters $s(\mu)$, which we may collectively denote as "outputs", are performance indexes for the particular input μ – for example stresses, velocity, flow rates. These outputs are typically expressed as functionals of field variables associated with a set of parametrized partial differential equations which describe the physical behavior of the system or its components. We are interested in calculating the outputs $s(\mu) = \mathcal{F}(\mu)$, for many different inputs/configurations μ chosen from a parameter space $\mathcal{D} \subset \mathbb{R}^P$, where P is the number of input parameters. Here, $\mathcal{F}$ encompasses the mathematical description of the physical problem. For the evaluation of $\mathcal{F}$ the underlying equations have to be solved. Usually, an analytical solution is not easy to obtain, rather a discretization procedure like the finite-element method, is used; then $\mathcal{F}$ is replaced by $\mathcal{F}_h$, a discrete form amenable to numerical solution. The basic premise, is that as the discretization "length" $h \to 0$, then $\mathcal{F}_h \to \mathcal{F}$, and consequently $s_h(\mu) \to s(\mu)$, $\forall \mu \in \mathcal{D}$ *but* as $h \to 0$ the cost of evaluating $\mathcal{F}_h$ becomes prohibitive. Especially in the context of design, control, or parameter identification where "real-time" response or many "input-output" evaluations are required, a balance between computational cost and accuracy/certainty is essential.
Identifying the problem in the high dimensionality of the discrete problems, model-order reduction techniques have been developed. The critical observation is that instead of using projection spaces with general approximation properties — like in finite element method— we choose problem-specific approximation spaces and use these for the discretization of the original problem. Using such spaces, we can construct a model that represents with sufficient accuracy the physical problem of interest using a significantly smaller number of degrees of freedom. Depending on the choice of the global approximation spaces many possible reductions are available.

The computational methods developed in this work permit *rapid* and *reliable* evaluation of this input-output relationship induced by partial differential equations *in the limit of many queries* — that is, in the design, optimization, control, and characterization contexts. In designing new methods, certain qualities must be considered:

- *Efficiency* is crucial for the problems in consideration. To achieve efficiency, we shall use the reduced-basis method; a weighted-residual Galerkin-type method, where the solution is projected onto low-dimensional spaces with certain problem-specific approximation properties.

- *Relevance.* Usually in a design or optimization procedure we are not interested in the field solution, but rather in certain design measures. The methods developed give accurate approximations to these outputs of interest, defined as functional outputs of the field solution.

- *Reliability.* To quantify the error introduced by the reduced-basis method, an error analysis must be invoked on outputs of interest.

In our field of interest, reduced basis approximation provides not only high computational savings, a rapid (real-time) and accurate methodological pre-process to detect the essential feature of the optimization process itself, but also the study of a geometrical sensitivity analysis of a complete bypass configuration. By selecting a limited number of relevant geometrical parameters (bypass diameter t, artery diameter D, stenosis length S, graft angle θ, bypass bridge height H, as reported in Figure 1) and a moderate number (N) of sample parameters

$$\boldsymbol{\mu}_k = \{t_k, D_k, S_k, \theta_k, H_k\},\ k = 1, \ldots, N,$$

we solve the parametrized equations that govern the physical problem in a reference domain Ω, properly mapped by coordinate transformations (see for a preliminary example [7]). This aspect is considered in Section 2. Then we build properly reduced basis functional approximation spaces for velocity and pressure to guarantee approximation and algebraic stability. For a new sample $\boldsymbol{\mu}_k$ we look for a new solution which is given by a weighted combination of previously computed and stored solutions. Weights are given by the solution of a state problem on the subspace of the reduced basis by a Galerkin projection. In this work reduced basis methods have been applied to Navier Stokes problem, used to model blood flow at moderate Reynolds (~ 1000). The most original contribution are concerned with the pressure treatment in Navier-Stokes problem, the introduction of geometrical parametrization of domain by non-affine maps, the study of different options to guarantee approximation stability of reduced basis approximation and, finally, basis orthonormalization to achieve algebraic stability for reduced basis (see [8] for more details). This methodological development highlights the great potential of reduced basis methods in optimal flow control and shape optimization, not only for pre-process optimization. Reduced basis can be seen as methods to solve in real-time complex problem with great computational savings without loosing accuracy and fast convergence.

2 REDUCED BASIS FOR STEADY NAVIER-STOKES EQUATIONS

The steady Navier-Stokes equations in a domain $\Omega \subset \mathbb{R}^d (d = 1, 2, 3)$ with boundary conditions $\Gamma = \Gamma_{in} \cup \Gamma_{out} \cup \Gamma_w$ are considered:

$$\begin{cases} -\nu\Delta\mathbf{u} + (\mathbf{u}\cdot\nabla)\mathbf{u} + \nabla p = \mathbf{f}\ in\ \Omega, \\ \nabla\cdot\mathbf{u} = 0\ in\ \Omega, \\ \mathbf{u} = \mathbf{0}\ on\ \Gamma_w;\ \mathbf{u} = \mathbf{g}_{in}\ on\ \Gamma_{in}, \left(\nu\frac{\partial\mathbf{u}}{\partial\hat{\mathbf{n}}} - p\hat{\mathbf{n}}\right) = \mathbf{0}\ on\ \Gamma_{out}, \end{cases} \tag{1}$$

where $\mathbf{u}$ is the velocity, p the pressure, $\mathbf{f}$ a force field, ν a kinematic viscosity and $\mathbf{n}$ the normal unit vector to the domain boundary. For the mathematical theory of the Navier-Stokes equations see e.g. [9] and for their numerical solution see [10], [11], [12].

The weak formulation of problem (1) reads: find $\mathbf{u} \in Y = (H^1_{\Gamma_D}(\Omega))^d,\ p \in Q = L^2(\Omega)$:

$$\begin{cases} \nu \int_\Omega \nabla \mathbf{u} \cdot \nabla \mathbf{w} d\Omega - \int_\Omega p \nabla \cdot \mathbf{w} d\Omega + \int_\Omega (\mathbf{u} \cdot \nabla)\mathbf{u} \cdot \mathbf{w} d\Omega = \int_\Omega \mathbf{f} \cdot \mathbf{w} d\Omega + \langle F^0, \mathbf{w} \rangle \ \forall \mathbf{w} \in Y, \\ \int_\Omega q \nabla \cdot \mathbf{u} d\Omega = \langle G^0, q \rangle \ \ \forall q \in Q, \end{cases} \tag{2}$$

F^0, G^0 are terms due to non-homogeneous Dirichlet boundary condition on Γ_{in}, $\Gamma_D = \Gamma_{in} \cup \Gamma_w$ and $H^1_{\Gamma_D}(\Omega) = \{v \in H^1(\Omega) :\ v = 0 \ on \ \Gamma_D\}$. We discretize problem (2) by a stable approximation using finite element method (e.g. the Taylor-Hood $\mathbb{P}^2 - \mathbb{P}^1$ elements for velocity and pressure, respectively) on a fine mesh triangulation; see, for example, [13]. The numerical methods used to solve the system of non-linear equations (2) is the iterative Newton method and involves the Frechet linerization of the advection term $(\mathbf{u}_h \cdot \nabla)\mathbf{u}_h$ considering its derivative in the *Frechet* sense. The linearized version of the discretized problem (2) at each iteration reads: given $\mathbf{u}_h^{(k)}$, find $\mathbf{u}_h^{(k+1)} \in Y_h,\ p_h^{(k+1)} \in Q_h$, such that

$$\begin{cases} \nu \int_\Omega \nabla \mathbf{u}_h^{(k+1)} \cdot \nabla \mathbf{w}_h d\Omega - \int_\Omega p_h^{(k+1)} \nabla \cdot \mathbf{w}_h d\Omega + \int_\Omega [(\mathbf{u}_h^{(k)} \cdot \nabla)\mathbf{u}_h^{(k+1)} + \\ + (\mathbf{u}_h^{(k+1)} \cdot \nabla)\mathbf{u}_h^{(k)}] \cdot \mathbf{w}_h \ d\Omega - \int_\Omega (\mathbf{u}_h^{(k)} \cdot \nabla)\mathbf{u}_h^{(k)} \cdot \mathbf{w}_h \ d\Omega = \\ = \int_\Omega \mathbf{f} \cdot \mathbf{w}_h d\Omega + \langle F^0, \mathbf{w}_h \rangle \ \forall \mathbf{w}_h \in Y_h, \\ \int_\Omega q_h \nabla \cdot \mathbf{u}_h^{(k+1)} d\Omega = \langle G^0, q_h \rangle \ \ \forall q_h \in Q_h, \end{cases} \tag{3}$$

2.1 Geometrical parametric dependence: the reference domain formulation

We suppose that the parametrized domain we are now considering is made of R components: $\hat{\Omega} = (\bigcup_{r=1}^R \bar{\hat{\Omega}}^r)$, so that we rewrite (3) as follows, introducing the "hat" notation to indicate equations in parametrized domains and dropping the subscript h for simplicity of notation:

$$\begin{cases} \hat{\mathcal{A}}(\hat{\mathbf{u}}^{(k+1)}, \hat{\mathbf{w}}) + \hat{\mathcal{B}}(\hat{p}^{(k+1)}, \hat{\mathbf{w}}) + \hat{\mathcal{C}}(\hat{\mathbf{u}}^{(k+1)}, \hat{\mathbf{u}}^{(k)}, \hat{\mathbf{w}}) + \hat{\mathcal{C}}(\hat{\mathbf{u}}^{(k)}, \hat{\mathbf{u}}^{(k+1)}, \hat{\mathbf{w}}) = \\ = \langle \hat{F}, \hat{\mathbf{w}} \rangle + \hat{\mathcal{C}}(\hat{\mathbf{u}}^{(k)}, \hat{\mathbf{u}}^{(k)}, \hat{\mathbf{w}}) \ \ \forall \hat{\mathbf{w}} \in \hat{Y}, \\ -\hat{\mathcal{B}}(\hat{q}, \hat{\mathbf{u}}^{(k+1)}) = \langle \hat{G}^0, \hat{q} \rangle \ \ \forall \hat{q} \in \hat{Q}, \end{cases} \tag{4}$$

where for $1 \le i, j \le d$ and $\hat{\nu}_{i,j} = \nu \delta_{i,j}$ (summation convention is understood):

$$\hat{\mathcal{A}}(\hat{\mathbf{u}}, \hat{\mathbf{w}}) = \sum_{r=1}^R \int_{\hat{\Omega}^r} \frac{\partial \hat{\mathbf{u}}}{\partial \hat{x}_i} \hat{\nu}_{ij} \frac{\partial \hat{\mathbf{w}}}{\partial \hat{x}_j} d\hat{\Omega}, \tag{5}$$

$$\hat{\mathcal{B}}(\hat{p}, \hat{\mathbf{w}}) = -\sum_{r=1}^R \int_{\hat{\Omega}^r} \hat{p} \nabla \cdot \hat{\mathbf{w}} d\hat{\Omega}, \tag{6}$$

$$\hat{\mathcal{C}}(\hat{\mathbf{u}},\hat{\mathbf{v}},\hat{\mathbf{w}}) = \sum_{r=1}^{R}\int_{\hat{\Omega}^r}(\hat{\mathbf{u}}\cdot\nabla)\hat{\mathbf{v}}\cdot\hat{\mathbf{w}}d\hat{\Omega}, \tag{7}$$

$$\langle\hat{F},\hat{\mathbf{w}}\rangle = \langle\hat{F}_s,\hat{\mathbf{w}}\rangle + \langle\hat{F}^0,\hat{\mathbf{w}}\rangle, \tag{8}$$

and

$$\langle\hat{F}_s,\hat{\mathbf{w}}\rangle = \sum_{r=1}^{R}\int_{\hat{\Omega}^r}\hat{\mathbf{f}}\hat{\mathbf{w}}d\hat{\Omega}, \langle\hat{F}^0,\hat{\mathbf{w}}\rangle = -\langle\hat{\mathcal{A}}\hat{\mathbf{g}}_{in},\hat{\mathbf{w}}\rangle,\ \langle\hat{G}^0,\hat{q}\rangle = \langle\hat{\mathcal{B}}\hat{q},\hat{\mathbf{g}}_{in}\rangle. \tag{9}$$

The problem now may be traced back to a *reference domain* by *non-affine mappings* on the different subdomains $\hat{\Omega}^r$ into Ω^r. For any $\hat{x}\in\hat{\Omega}^r$, $r=1,\ldots,R$, its image $x\in\Omega^r$ is given by:

$$x = T^r(\mu;\hat{x}) + g^r,\quad 1\le r\le R, \tag{10}$$

thus

$$\frac{\partial}{\partial\hat{x}_i} = \frac{\partial x_j}{\partial\hat{x}_i}\frac{\partial}{\partial x_j} = T^r_{ji}(\mu,x)\frac{\partial}{\partial x_j}. \tag{11}$$

In the reference domain Ω we have:

$$\mathcal{A}(\mu;\mathbf{u},\mathbf{w}) = \sum_{r=1}^{R}\int_{\Omega^r}\frac{\partial\mathbf{u}}{\partial x_i}\nu^r_{ij}(\mu,x)\frac{\partial\mathbf{w}}{\partial x_j}d\Omega\ \forall\mathbf{w}\in Y, \tag{12}$$

$$\mathcal{B}(\mu;p,\mathbf{w}) = -\sum_{r=1}^{R}\int_{\Omega^r}p\chi^r_{ij}(\mu,x)\frac{\partial w_j}{\partial x_i}d\Omega\ \forall\mathbf{w}\in Y, \tag{13}$$

$$\mathcal{C}(\mu;\mathbf{u},\mathbf{v},\mathbf{w}) = -\sum_{r=1}^{R}\int_{\Omega^r}u_i\pi^r_{ij}(\mu,x)\frac{\partial v_j}{\partial x_i}\mathbf{w}d\Omega\ \forall\mathbf{w}\in Y, \tag{14}$$

$$\langle F,\mathbf{w}\rangle = \langle F_s,\mathbf{w}\rangle + \langle F^0,\mathbf{w}\rangle, \tag{15}$$

where

$$\langle F_s,\mathbf{w}\rangle = \sum_{r=1}^{R}\int_{\Omega^r}\left(\hat{\mathbf{f}}^r det(T^r(\mu,x))^{-1}\right)\mathbf{w}d\Omega; \tag{16}$$

$$\langle F^0,\mathbf{w}\rangle = -\langle\mathcal{A}\mathbf{g}_{in},\mathbf{w}\rangle;\ \langle G^0,q\rangle = \langle\mathcal{B}q,\mathbf{g}_{in}\rangle.$$

The *transformation tensors* for viscous bilinear forms are defined as follows:

$$\nu^r_{ij}(\mu,x) = T^r_{ii'}(\mu,x)\hat{\nu}_{i'j'}T^r_{jj'}(\mu,x)det(T^r(\mu,x))^{-1}, 1\le i,j\le d, r=1,...,R. \tag{17}$$

The tensors for *pressure, divergence and advection forms* are defined, as:

$$\chi^r_{ij}(\mu,x) = \pi^r_{ij}(\mu,x) = T^r_{ij}(\mu,x)det(T^r(\mu,x))^{-1}. \tag{18}$$

2.2 The empirical interpolation method

We are considering subdomains characterized by a non-affine parametric dependence. We apply, as already proposed in [14] and [15], an empirical interpolation procedure to expand non-affine mapping terms and decouple the parameters dependent contribution from the one depending only on spacial coordinates (computed once on a reference domain). Let us recall the algorithm based on the empirical interpolation method. We consider a generic function $g(x,\mu)$ representing the non-affine mapping term (e.g describing a shape). The goal is to develop:

$$g_M(x,\mu) = \Sigma_{m=1}^{M}\beta_m(\mu)q_m(x), \tag{19}$$

as a sum of products decomposed in two parts: $\beta_m(\mu)$ are parameters dependent weights (computed many times for each value of μ); $q_m(x)$ are shape functions without a parametric dependence (computed only once).
The main elements are the test "shape" functions and the interpolation points, respectively:

$$W_M^g = \{\gamma_m = g(.,\mu_m^g), 1 \le m \le M\}, \mu_m^g \; properly \; chosen,$$
$$\mathcal{T}_M = \{t_1, \dots t_M\}, 1 \le M \le M_{max}, \; sets \; of \; interpolation \; points.$$

The interpolation algorithm is:

$$for \; M = 1, set \; t_1 = argsup_{x\in\Omega}|\gamma_1(x)|, \; q_1 = \gamma_1(x)/\gamma_1(t_1), (off-line)$$
$$then, \; for \; M = 2, \dots, M_{max}: \; \Sigma_{j=1}^{M-1}\sigma_j^{M-1}q_j(t_i) = \gamma_M(t_i), 1 \le i \le M-1, (off-line)$$
$$r_M(x) = \gamma_M(x) - \Sigma_{j=1}^{M-1}\sigma_j^{M-1}q_j(x), t_M = argsup_{x\in\Omega}|r_M(x)|, (off-line)$$
$$q_M(x) = r_M(x)/r_M(t_M); g_M(x,\mu) = \Sigma_{m=1}^{M}\beta_m(\mu)q_m(x), (off-line)$$
$$\Sigma_{j=1}^{M}q_j(t_i)\beta_j(\mu) = g(t_i,\mu), 1 \le i \le M, \; (on-line).$$

To stop the procedure we impose $\|g(.,\mu) - g_M(.,\mu)\|_{L^\infty(\Omega)} \le \epsilon_{max}$ where ϵ_{max} is an interpolation error. By applying the algorithm recalled above we may write:

$$\nu_{ij}^r(\mu,x) = \Sigma_{m=1}^{M_{ijr}^a}\beta_{ijm}^r(\mu)\gamma_{ijm}^r(x), \tag{20}$$

$$\chi_{ij}^r(\mu,x) = \Sigma_{m=1}^{M_{ijr}^b}\alpha_{ijm}^r(\mu)\omega_{ijm}^r(x), \tag{21}$$

where m refers to the number of interpolation functions we use for each form (related with max interpolation error), i and j are indexes related to linear/bilinear form, r is the subdomain index, β and α are weighting quantities depending on the parameters μ, γ and ω are the interpolation functions used as basis. Furthermore, we define

$$\Psi^{t(i,j,r,m)}(\mu) = \beta_{ijm}^r(\mu), \; \mathcal{A}^{t(i,j,r,m)}(\gamma(x),\mathbf{u},\mathbf{w}) = \int_{\Omega^r}\gamma_{ijm}^r(x)\frac{\partial\mathbf{u}}{\partial x_i}\frac{\partial\mathbf{w}}{\partial x_j}d\Omega, \tag{22}$$

$$\Upsilon^{p(i,j,r,m)}(\mu) = \alpha^r_{ijm}(\mu),\ \mathcal{B}^{p(i,j,r,m)}(\omega(x), p, \mathbf{w}) = -\int_{\Omega^r} \omega^r_{ijm}(x) p \frac{\partial w_i}{\partial x_j} d\Omega, \tag{23}$$

$$\mathcal{C}^{p(i,j,r,m)}(\omega(x), \mathbf{u}, \mathbf{v}, \mathbf{w}) = \int_{\Omega^r} \omega^r_{ijm}(x) u_i \frac{\partial v_i}{\partial x_j} \mathbf{w} d\Omega, \tag{24}$$

for $1 \leq r \leq R$, $1 \leq i, j \leq d$, $1 \leq m \leq max(M^a_{ijr}, M^b_{ijr})$ (t and p are condensed indexes of i, j, r, m quantities used to simplify notation: each value of t or p represents a different combination of the previous four indexes i, j, r, m). We may now apply an *effectively affine* decomposition to the following operators:

$$\mathcal{A}(\mu, \mathbf{u}, \mathbf{w}) = \sum_{t=1}^{Q^a} \Psi^t(\mu) \mathcal{A}^t(\gamma(x), \mathbf{u}, \mathbf{w});$$

$$\mathcal{B}(\mu, p, \mathbf{w}) = \sum_{p=1}^{Q^b} \Upsilon^p(\mu) \mathcal{B}^p(\omega(x), p, \mathbf{w}) \ ;$$

$$\mathcal{C}(\mu, \mathbf{u}, \mathbf{v}, \mathbf{w}) = \sum_{p=1}^{Q^c} \Upsilon^p(\mu) \mathcal{C}^p(\omega(x), \mathbf{u}, \mathbf{v}, \mathbf{w}) \ ;$$

in general, being $\Omega \subset \mathbb{R}^d$, $Q^a = \Sigma^d_{j=1}\Sigma^d_{i=1}\Sigma^R_{r=1} M^a_{ijr}$; $Q^b = \Sigma^d_{j=1}\Sigma^d_{i=1}\Sigma^R_{r=1} M^b_{ijr}$ and $Q^c = \Sigma^d_{j=1}\Sigma^d_{i=1}\Sigma^R_{r=1} M^b_{ijr}$;

The non-linear problem (2) has to be discretized, then linearized to be solved by an iterative method. This problem has an inf-sup condition (LBB) [13] to be guaranteed:

$$\beta(\mu) = \inf_{q \in Q} \sup_{\mathbf{w} \in Y} \frac{\mathcal{B}(\mu, q, \mathbf{w})}{\|\mathbf{w}\|_Y \|q\|_Q} \geq \beta_0 > 0, \forall\ \mu\ \in\ \mathcal{D};$$

We introduce the supremizer operator T^μ: $Q \to Y$ so that

$$(T^\mu q, \mathbf{w})_Y = \mathcal{B}(\mu; q, \mathbf{w}),\ \forall\ \mathbf{w}\ \in\ Y \tag{25}$$

and

$$T^\mu q = \arg \sup_{\mathbf{w} \in Y} \frac{\mathcal{B}(\mu; q, \mathbf{w})}{\|\mathbf{w}\|_Y},$$

then

$$\beta^2(\mu) = \inf_{q \in Q} \frac{(T^\mu q, T^\mu q)_Y}{\|q\|^2_Q}.$$

2.3 Reduced Basis Formulation

In the reduced basis approximation we choose properly (i.e. by optimized algorithm as proposed for example in [16] if we want to improve computing performance) a set of sample parameters $S_N^{\boldsymbol{\mu}} = \{\boldsymbol{\mu}^1, \ldots, \boldsymbol{\mu}^N\}$, where $\boldsymbol{\mu}^n \in \mathcal{D}^\mu$, $n = 1, \ldots, N$.
Correspondingly, we take a set of couples $(\mathbf{u}_h(\mu^n), p_h(\mu^n))$ which are approximate solutions of the Navier-Stokes problem (3) using finite element method. Then we build approximation spaces: the *reduced basis pressure space* is $Q_N = \text{span}\,\{\xi_n,\ n = 1, \ldots, N\}$, where $\xi_n = p_h(\mu^n)$, while for the *reduced basis velocity space* we enrich the basis solving problem (25) with finite element method and computing supremizer solutions. We build a velocity space which is μ dependent, and for this reason assembled on-line:
$Y_N^\mu = \text{span}\,\{\zeta_n,\ n = 1, \ldots, N; T^\mu \xi_n,\ n = 1, \ldots, N\}$, where $\zeta_n = \mathbf{u}_h(\mu^n)$. More details will follow.
The reduced basis approximation problem reads: find $(\mathbf{u}_N(\mu), p_N(\mu)) \in Y_N \times Q_N$ s.t.:

$$\begin{cases} \mathcal{A}(\mu; \mathbf{u}_N(\mu), \mathbf{w}) + \mathcal{B}(\mu; p_N(\mu), \mathbf{w}) + \mathcal{C}(\mu; \mathbf{u}_N(\mu), \mathbf{u}_N(\mu), \mathbf{w}) = \langle F, \mathbf{w} \rangle \ \forall\ \mathbf{w} \in\ Y_N, \\ \mathcal{B}(\mu; q, \mathbf{u}_N(\mu) = \langle G^0, q \rangle \ \forall\ q \in\ Q_N. \end{cases} \tag{26}$$

This problem does admit an inf-sup property. We introduce

$$\beta_N(\mu) = \inf_{q \in Q_N} \sup_{\mathbf{w} \in Y_N} \frac{\mathcal{B}(\mu, q, \mathbf{w})}{\|\mathbf{w}\|_Y \|q\|_Q},$$

and supremizer solutions allow to guarantee the following stability condition:

$$\beta_N(\mu) \geq \beta_h(\mu) \geq \beta_0 > 0, \forall \mu \in \mathcal{D}^\mu,$$

where β_h is the inf-sup constant associated with the Galerkin method. For further elements dealing supremizer operator and the reduced basis framework see [16]. We rewrite for computational convenience Y_N^μ using the *effectively affine dependence* of $\mathcal{B}(\mu; q, \mathbf{w})$ on the parameter and the *linearity* of T^μ (allowing to assemble velocity reduced basis space on-line):

$$T^\mu \xi = \sum_{p=1}^{Q^b} \Upsilon^p(\mu) T^p \xi \tag{27}$$

for any ξ and μ, where:

$$(T^p \xi, \mathbf{w})_Y = \mathcal{B}^p(\omega, q, \mathbf{w}) \ \forall\ \mathbf{w}\ \in\ Y,$$

which allows us to write:

$$Y_N^\mu = \text{span}\,\{\sum_{k=1}^{Q^b}\ \Upsilon^k(\mu)\sigma_{kn}, n = 1, \ldots, 2N\},$$

where $\overline{Q}^b = Q^b + 1, \Upsilon^{\overline{Q}^b} = 1$.
For $n = 1, \ldots, N$:

$$\sigma_{kn} = 0, for\ k = 1, \ldots, Q^b;$$

$$\sigma_{\overline{Q}^b n} = \zeta_n = \mathbf{u}_h(\mu^n).$$

For $n = N+1, \ldots, 2N$:

$$\sigma_{\overline{Q}^b n} = 0;$$

$$(\sigma_{kn}, \mathbf{w})_Y = \mathcal{B}^k(\omega, \xi_{n-N}, \mathbf{w}), \forall \mathbf{w} \in Y, for\ k = 1, \ldots, Q^b. \tag{28}$$

For a new "μ" we want a solution given by a combination of previously computed stored solutions as basis functions, i.e.:

$$\mathbf{u}_N(\mu) = \sum_{j=1}^{2N} u_{Nj}(\mu) \Big(\sum_{k=1}^{\overline{Q}^b} \Upsilon^k(\mu) \boldsymbol{\sigma}_{kj} \Big),$$

$$p_N(\mu) = \sum_{l=1}^{N} p_{Nl}(\mu) \xi_l,$$

whose unknowns u_{Nj} and p_{Nl} satisfy the following non-linear system:

$$\begin{cases} \sum_{j=1}^{2N} A_{ij}^{\mu} \mathbf{u}_{Nj}(\mu) + \sum_{l=1}^{N} B_{il}^{\mu} p_{Nl}(\mu) + \sum_{h=1}^{2N} \sum_{j=1}^{2N} \mathbf{u}_{Nh}(\mu) C_{ijh}^{\mu} \mathbf{u}_{Nj}(\mu) = F_i, \quad 1 \le i \le 2N, \\ \sum_{j=1}^{2N} B_{jl}^{\mu} \mathbf{u}_{Nj}(\mu) = G_l, \quad 1 \le l \le N. \end{cases} \tag{29}$$

To solve it we apply the Newton method which reads, yielding the following iteration: for $k \ge 0$ given $\mathbf{u}_{Nj}^{(k)}$, find $\mathbf{u}_{Nj}^{(k+1)}$ and $p_{Nl}^{(k+1)}$ such that

$$\begin{cases} \sum_{j=1}^{2N} A_{ij}^{\mu} \mathbf{u}_{Nj}^{(k+1)}(\mu) + \sum_{l=1}^{N} B_{il}^{\mu} p_{Nl}^{(k+1)}(\mu) + \sum_{h=1}^{2N} \sum_{j=1}^{2N} \mathbf{u}_{Nh}^{(k)}(\mu) C_{ijh}^{\mu} \mathbf{u}_{Nj}^{(k+1)}(\mu) + \\ + \sum_{h=1}^{2N} \sum_{j=1}^{2N} \mathbf{u}_{Nh}^{(k+1)}(\mu) C_{ijh}^{\mu} \mathbf{u}_{Nj}^{(k)}(\mu) = F_i^{\mu} + \sum_{h=1}^{2N} \sum_{j=1}^{2N} \mathbf{u}_{Nj}^{(k)}(\mu) C_{ijh}^{\mu} \mathbf{u}_{Nh}^{(k)}(\mu) \\ \sum_{j=1}^{2N} B_{jl}^{\mu} \mathbf{u}_{Nj}^{(k+1)}(\mu) = G_l^{\mu}, \quad 1 \le l \le N, \ 1 \le i \le 2N. \end{cases} \tag{30}$$

The sub-matrices A, B and C are given by:

$$A_{ij}^{\mu} = \sum_{z=1}^{Q^a} \sum_{k'=1}^{\overline{Q}^b} \sum_{k''=1}^{\overline{Q}^b} \Psi^z(\mu) \Upsilon^{k'}(\mu) \Upsilon^{k''}(\mu) \mathcal{A}^z(\gamma, \sigma_{k'i}, \sigma_{k''j}), \ 1 \le i, j \le 2N;$$

$$B_{il}^{\mu} = \sum_{z=1}^{Q^b} \sum_{k'=1}^{\overline{Q}^b} \Upsilon^z(\mu) \Upsilon^{k'}(\mu) \mathcal{B}^z(\omega, \sigma_{k'i}, \xi_l), \ 1 \le i \le 2N, \ 1 \le l \le N;$$

$$C_{ijh}^{\mu} = \sum_{z=1}^{Q^c} \sum_{k'=1}^{\overline{Q}^b} \sum_{k''=1}^{\overline{Q}^b} \sum_{k'''=1}^{\overline{Q}^b} \Upsilon^k(\mu) \Upsilon^{k'}(\mu) \Upsilon^{k''}(\mu) \Upsilon^{k'''}(\mu) \mathcal{C}^z(\omega, \sigma_{k'i}, \sigma_{k'j}, \sigma_{k'h}), \ 1 \le i, j, h \le 2N;$$

$$F_i = \sum_{k'=1}^{\overline{Q}^b} \Upsilon^{k'}(\mu)\langle F, \sigma_{k'i}\rangle,\ 1 \le i \le 2N;$$

$$G_l = \langle G^0, \xi_l\rangle,\ 1 \le l \le N.$$

In compact form the linearized problem (30) can therefore be written as:

$$\begin{pmatrix} \underline{A} + \underline{C}^{(k+1)} & \underline{B} \\ \underline{B}^T & 0 \end{pmatrix} \cdot \begin{pmatrix} \underline{\mathbf{u}}_N^{(k+1)} \\ \underline{p}_N^{(k+1)} \end{pmatrix} = \begin{pmatrix} \underline{F}^{(k)} \\ \underline{G} \end{pmatrix}. \tag{31}$$

By accounting also for the computation of supremizer components in the velocity space the following number of operations is needed in order to build reduced basis matrices: $O(Q^a(\overline{Q}^b)^2 4N^2)$ for sub-matrix $\underline{A}$, $O((\overline{Q}^b)^2 2N^2)$ for $\underline{B}$, $O(Q^c(\overline{Q}^b)^3 8N^3)$ for $\underline{C}$, $O(\overline{Q}^b N)$ for $\underline{F}$ and $O(N^3)$ for the "inversion" of the full reduced basis matrix (31) at each Newton iteration. The quantities Q^a, Q^b and Q^c are depending on the number of "shape functions" ($\gamma(x)$ and $\omega(x)$) related with interpolation error (ε_{max}) and the number of subdomains with non-affine mappings (R). Other options to build reduced basis spaces, where stability can be theoretically proven, are available (see for example [8]) to get a different space Y_N for velocity. For example: i) a space which is $\boldsymbol{\mu}$-independent, using only $T^q\xi$ components to enrich velocity space. This option is useful if we want to apply an orthonormalization procedure to restore algebraic stability; or ii) a space $\boldsymbol{\mu}$-independent, using the offline value of the parameter μ^i in $\Upsilon^q(\mu^i)$.

3 THE BYPASS PROBLEM

We consider the parametrized bypass configuration as represented in Figure 3 with the vector of parameters $\boldsymbol{\mu} = \{t, D, L, S, H, \theta, \upsilon\} \in \mathcal{D}^\mu \subset \mathbb{R}^P$ with $\mathcal{D}^\mu$ given by: $[t_{min}, t_{max}] \times [D_{min}, D_{max}] \times [L_{min}, L_{max}] \times [S_{min}, S_{max}] \times [H_{min}, H_{max}] \times [\theta_{min}, \theta_{max}] \times [\upsilon_{min}, \upsilon_{max}]$. This test problem deals with non-affine parameters dependence. The aim is to study the same non-linear problem by varying different geometrical parameters and then to test reduced basis convergence, extract output information and a sensitivity analysis on parameters of interest. Referring to notation in Section 2 we consider $R = 4$. The coordinate transformation in Ω^1 with non-affine parametric dependence is given by:

$$\begin{cases} x_1 = \frac{1}{H}\hat{x}_1 \\ x_2 = \frac{1}{t}(\hat{x}_2 - (\upsilon H^2 x_1(x_1 - 1) + H x_1 \tan(\theta))). \end{cases} \tag{32}$$

The role of parameters t and H is to stretch subdomain Ω^1 (as L, S, D stretch the remaining subdomains), the parameter υ introduces a curvature in the walls of the incoming branch of the bypass and θ is responsible for a rigid rotation by letting the graft angle vary. In this way we may separate a subdomain (i.e Ω^1) where we have a complex non-affine parametric dependence from other subdomains where the parametric dependence

is simpler (i.e. $\Omega^2, \Omega^3, \Omega^4$), thus improving computational efficiency of the method. The tensors for *viscous bilinear terms* are given by:

$$\nu^1 = \nu \left[\begin{array}{cc} \frac{t}{H} & -(\tan\theta + 2\upsilon H x_1 - \upsilon H) \\ -(\tan\theta + 2\upsilon H x_1 - \upsilon H) & \frac{(1+(\tan\theta+2\upsilon H x_1 - \upsilon H)^2)}{t} H \end{array} \right]; \tag{33}$$

$$\nu^2 = \nu \left[\begin{array}{cc} \frac{S}{D} & 0 \\ 0 & \frac{D}{S} \end{array} \right]; \nu^3 = \nu \left[\begin{array}{cc} \frac{t}{D} & 0 \\ 0 & \frac{D}{t} \end{array} \right]; \ \nu^4 = \nu \left[\begin{array}{cc} \frac{L}{D} & 0 \\ 0 & \frac{D}{L} \end{array} \right]. \tag{34}$$

The tensors for *pressure, divergence and transport terms* are given by:

$$\chi^1 = \pi^1_T = \left[\begin{array}{cc} t & -H(\tan\theta + 2\upsilon H x_1 - \upsilon H) \\ 0 & H \end{array} \right]; \ \chi^2 = \pi^2_G = \left[\begin{array}{cc} S & 0 \\ 0 & D \end{array} \right]; \tag{35}$$

$$\chi^3 = \pi^3_G = \left[\begin{array}{cc} t & 0 \\ 0 & D \end{array} \right]; \ \chi^4 = \pi^4_G \left[\begin{array}{cc} L & 0 \\ 0 & D \end{array} \right]. \tag{36}$$

We apply empirical interpolation expansion to the components of tensors ν^1, χ^1 and π^1 and we build the reduced basis approximation spaces for velocity and pressure as seen in the previous section.

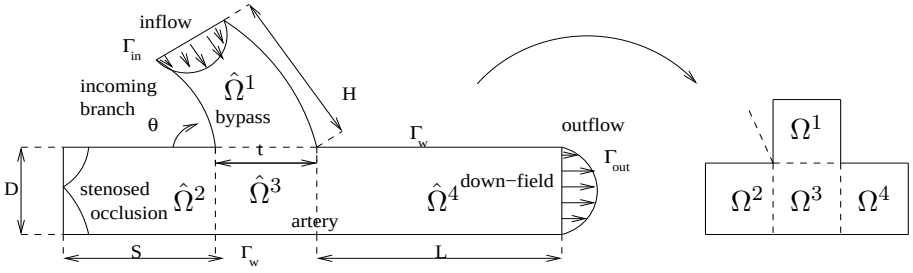

Figure 3: Geometrical scheme for the bypass test problem (physical domain and reference one).

We have carried out some tests based on the same geometry considering five different varying parameters (we have frozen L and H because less important). In particular we are interested in varying graft angle θ and curvature υ (defining the upstream geometry) and the ratio $\frac{t}{D}$. For preliminary results see [17]. In Figures 4 and 5 we report numerical results (max and mean relative H^1 errors on velocity and relative L^2 errors for pressure, comparing reduced basis surrogate solutions and the finite element ones) considering several different geometrical configurations varying N for two different maximum interpolation error $\varepsilon_{max} = 10^{-5}$ and then $\varepsilon_{max} = 10^{-8}$, to avoid to have interpolation error dominating our approximation with the constant "plateau" in error plots, by affecting the efficiency of our reduced basis approximation. Concerning computational costs, once all the off-line calculations are performed and data stored, the on-line costs are for the maximum N considered and shown in the pictures less than 10% if compared with the computational costs involved in finite element calculations (without considering the further costs of re-meshing).

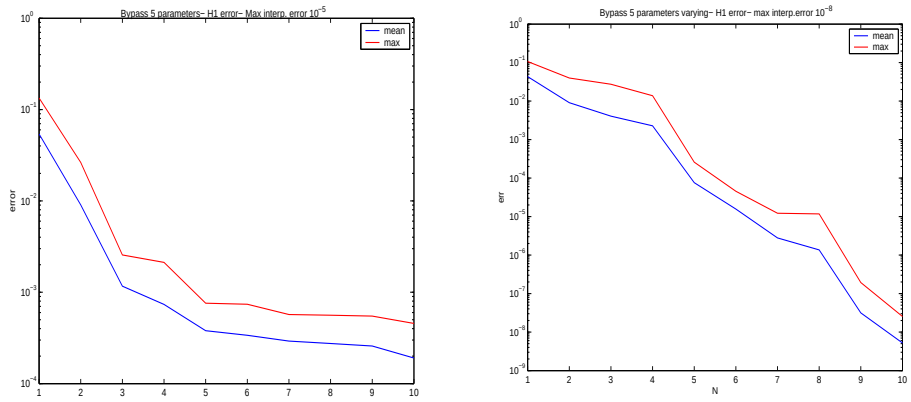

Figure 4: H^1 relative errors on velocity with different ϵ_{max} interpolation error imposed on all $g_M^j(x,\mu)$ (testing hundreds of different configurations with 5 different parameters varying).

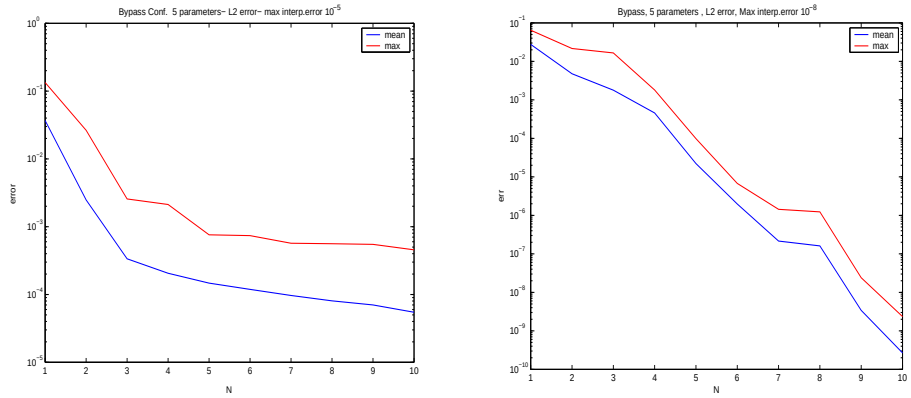

Figure 5: L^2 relative errors on pressure with different ϵ_{max} interpolation error imposed on all $g_M^j(x,\mu)$ (testing hundreds of configurations with 5 different parameters varying).

3.1 Outputs sensitivities

We conclude this section with some considerations about the influence of curvature of the upper stream geometry. The ratio $\frac{t}{D}$ is the most important parameter and it is responsible of recirculation in the host artery (see [17]), but also curvature has a role (see [8]). The ratio $\frac{S}{D}$ becomes important if we freeze $\frac{t}{D}$ and so the graft angle θ.
Figure 6 (left) shows the vorticity functional output, defined as $s(\mu) = \int_{\Omega_d}(\frac{\partial u_2}{\partial x_1} - \frac{\partial u_1}{\partial x_2})d\Omega$ varying the ratio $\frac{t}{D}$. We can see that if the ratio $\frac{t}{D}$ is less than unity (as usually is) vorticity is contained, otherwise if the bypass diameter t is larger with respect to the arterial diameter D a strong recirculation arises in the host vessel and also vorticity increases considerably. Usually the value of the quantity $\frac{t}{D}$ is in the range $[0.85 - 0.96]$.
Figure 6 (right) shows the behavior of vorticity varying the curvature of the upstream (inflow) geometry. Increasing the curvature υ the vorticity diminishes: this behavior can be explained by the fact that curvature is guiding the flow more smoothly. An interesting

analysis can be obtained introducing the *Dean* number, representing the ratio of the square root of the product of the inertial and centrifugal forces to the viscous forces, defined as follows

$$De = 4\Big[\frac{D}{R}\Big]^{\frac{1}{2}} Re, \tag{37}$$

where R is the radius of curvature and Re the Reynolds number. See also [18]. If we do not have curvature the Dean number is equal to zero. In the case we have considered, the range of the Dean number was $[0, 2.31 \cdot Re]$. By increasing the Dean number (and so *curvature*, the inverse of the curvature radius) makes the maximum of the $2D$ velocity profile to increase, but at the same time this maximum is displaced away from the center of curvature. Note that $De = 0$ corresponds to a case in which we have a centered velocity profile of *Hagen-Poiseuille* type. In our case the displacement of the peak velocity profile allows the blood to be driven into the host vessel more smoothly and to better adapt the upstream inflow condition at the junction geometry. In our case the critical zone of the bypass near the upper wall has lower mean velocity. Results in Figure 6 (right) refers to a graft angle of 45 degree and a ratio $\frac{t}{D} = 1$.

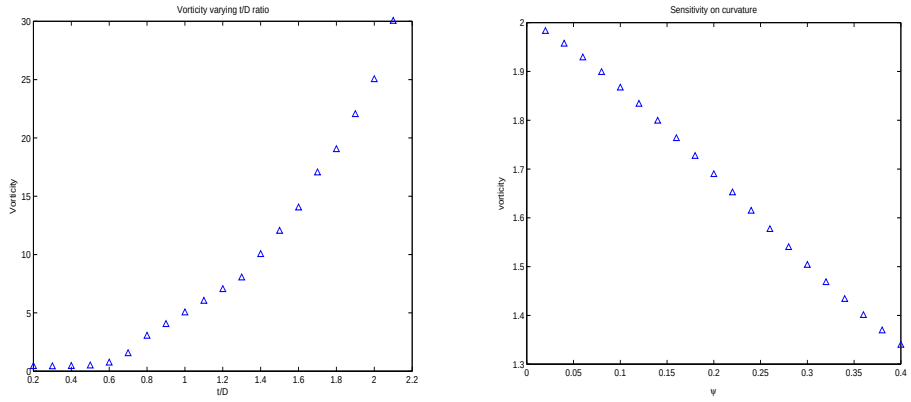

Figure 6: Distributed vorticity $[m^2 s^{-1}]$ varying $\frac{t}{D}$ (left); distributed vorticity $[m^2 s^{-1}]$ and curvature (right).

4 CONCLUSION

We have extended the use of reduced basis methodology to non-linear problems in domains with non-affine parametric dependence. This extension has allowed us to approximate flows in parametrized domains, e.g. blood flows in arterial bypasses, depending on geometrical parameters, by providing a sensitivity analysis for relevant geometrical and physical quantities. The goal of this investigation has been to provide a pre-process optimization tool to extract relevant information on bypass system and use them in applying more complex optimization tool such as optimal flow control in already optimized bypass configurations. When we are considering problems with an increasing complexity, such

as the ones with non-linearities and non-affine parametrization, the use of reduced basis method becomes even more competitive and computational savings are more relevant. Research guidelines are devoted in developing a posteriori error bounds for reduced basis in problems with geometrical parametric dependence. Other joint perspectives are the study of transient flows and fluid-structure interaction problems. Another approach with reduced basis for Navier-Stokes problem is provided in [19] where basis function are computed using spectral methods in each subdomains considering a technique called "reduced basis element method".

REFERENCES

[1] A. Quarteroni, L. Formaggia. *Mathematical Modelling and Numerical Simulation of the Cardiovascular System* in Modelling of Living Systems, Handbook of Numerical Analysis Series (P.G. Ciarlet e J.L. Lions Eds), Elsevier, Amsterdam, 2004.

[2] A. Quarteroni, G. Rozza. *Optimal control and shape optimization in aorto-coronaric bypass anastomoses. M^3AS*, Mathematical Models and Methods in Applied Sciences, Vol.13, No. 12 (2003), pp. 1801–23.

[3] V.I. Agoshkov, A. Quarteroni, G. Rozza. *Shape design approach using perturbation theory for bypass anastomoses*. Vol. 44, No. 1 (2006), pp.367-384.

[4] V.I. Agoshkov, A. Quarteroni, G. Rozza. *A Mathematical approach in the design of arterial bypass using unsteady Stokes equations.* In press (on-line) in Journal of Scientific Computing, (2006).

[5] C. Prud'homme, D. Rovas, K. Veroy, Y. Maday, A.T. Patera and G. Turinici. *Reliable real-time solution of parametrized partial differential equations: reduced-basis output bound methods*. J. Fluids Engineering, Vol. 172 (2002), pp. 70–80.

[6] G. Rozza. *On optimization, control and shape design of an arterial bypass.* International Journal for Numerical Methods in Fluids, Vol. 47, No. 10-11 (2005), pp. 1411–1419.

[7] G. Rozza. *Reduced basis methods for elliptic equations in sub-domains with a posteriori error bounds and adaptivity.* Applied Numerical Mathematics, Vol. 55, No. 4 (2005), pp. 403–424.

[8] G. Rozza, *Shape Design by Optimal Flow Control and Reduced Basis Techniques: Applications to Bypass Configurations in Haemodynamics*. PhD Thesis No.3400, Ecole Polythéchnique Fédérale de Lausanne, 2005.

[9] G.P. Galdi. *An Introduction to the Mathematical Theory of the Navier-Stokes Equations, Volume II: Nonlinear Steady Problem.* Springer-Verlag, New York, 1994.

[10] R. Temam. *Navier-Stokes Equations: Theory and Numerical Analysis*. North-Holland, Amsterdam, 1984.

[11] V. Girault, P.A. Raviart. *Finite Element Methods for Navier-Stokes Equations.* Springer-Verlag, Berlin, 1986.

[12] F. Brezzi, M. Fortin. *Mixed and Hybrid Finite Element Methods.* Springer and Verlag, New York, 1991.

[13] A. Quarteroni, A. Valli. *Numerical Approximation of Partial Differential Equations*. Springer-Verlag, Berlin, 1994.

[14] M. Barrault, Y. Maday, N.C. Nguyen and A.T.Patera. *An "empirical interpolation" method: application to efficient reduced-basis discretization of partial differential equations*. C. R. Acad. Sci. Paris, Analyse Numerique, Serie I, 2004, Vol. 339, pp. 667–672.

[15] G. Rozza. *Reduced basis methods for Stokes equations in domains with non-affine parameter dependence.* EPFL-IACS report 06.2005, submitted to Comp.Vis.Science.

[16] G. Rozza, K. Veroy. *On the stability of reduced basis methods for Stokes equations in parametrized domains*. Submitted, 2006.

[17] G. Rozza. *Real time reduced basis techniques for arterial bypass geometries.* In K.J. Bathe (ed.), Computational Fluid and Solid Mechanics, Elsevier, 2005, pp. 1283–1287.

[18] S.J. Sherwin, D.J. Doorly. *Flow dynamics within model distal arterial bypass graft.* Advances in Fluid Mechanics, Vol. 34 (2003), pp. 327–374.

[19] A.E. Løvgren. *Reduced Basis Modelling of Hierchical Flow Systems*. PhD Thesis, Norwegian University of Science and Technology, Trondheim, 2005.